BIOLOGY, MEDICINE, & NATURAL PRODUCT CHEMISTRY ISSN 2089-6514 (paper)
Volume 15, Number 1, April 2026 | Pages: 535-553 | DOI: 10.14421/biomedich.2026.151.535-553 ISSN 2540-9328 (online)

Bioinformatics Analysis of Quercetin and Morin Bioactivity from *Morinda citrifolia L.* Targeting *Streptococcus mutans* Virulence Factors In Dental Caries Cases

Astrid Ekklesia Saputri[1], Rian Ka Praja[2]*, Agnes Frethernety[3], Oktaviani Naulita Turnip[2], Ysrafil[3]
[1]Faculty of Medicine; [2]Departement of Microbiology, Faculty of Medicine; [3]Departement of Pharmacology, Faculty of Medicine, Universitas Palangka Raya
Jl. H. Timang, Palangka Raya, Indonesia.

Corresponding author*
riankapraja@med.upr.ac.id

Manuscript received: 16 December 2025. Revision accepted: 13 April 2026, Published: 18 May 2026.

Abstract

Dental caries remains one of the most neglected oral diseases, particularly among populations living far from healthcare services. Its pathogenesis is largely triggered by poor oral hygiene and the activity of *Streptococcus mutans*. The use of synthetic antimicrobial agents often leads to prolonged side effects and a higher risk of antibiotic resistance. As an alternative, *Morinda citrifolia L.* extract shows high potential due to its good public acceptance, minimal side effects, and proven in vitro efficacy in inhibiting *S. mutans* growth. This study aimed to investigate the bioactivity factors of *S. mutans* in relation to specific components of *Morinda citrifolia L.* as an alternative therapeutic agent for dental caries using a bioinformatics-based approach. A descriptive-exploratory bioinformatics method was employed using computational analysis. The bacterial FASTA sequence of *Streptococcus mutans* UA159 was retrieved from the National Center for Biotechnology Information (NCBI) database and analyzed using several software tools, including STITCH v5.0, VICMPred, VirulentPred, BepiPred v1.0, MHC I and MHC II BindingPred, and PSORTb v3.0. The analysis revealed notable interactions in bioactivity between *S. mutans* proteins and the phytocompounds quercetin and morin. Seven virulent proteins PknB, SMU_1806, SMU_1213c, SMU_922, SMU_906, SMU_525, and SMU_1078c, contribute to cellular process, metabolism, virulence factors, and information & storage. Five proteins were identified in the cytoplasmic membrane, one in cell wall, and also cytoplasm. Quercetin and morin demonstrated strong antibacterial potential against *S. mutans* through interactions with virulent proteins. PknB, SMU_906, and SMU_1078c stand out in epitope T cell analysis with high affinity, demonstrating the ability to provoke an adaptive immune system response. Location complexity of 5'-nucleotide enzyme targeted by strategic antimicrobials leads to bacterial mortality.

Keywords: Bioinformatics; Morin; Quercetin; *Streptococcus mutans*; virulence factors.

Abbreviations: ATP = Adenosine Triphosphate, BepiPred = B-epitope Prediction, FASTA = Fast Adaptive Shrinkage Threshold Algorithm; IUPAC = International Union of Pure and Applied Chemistry; MHC = Major Histocompatibility Complex; MIC = Minimum Inhibitory Concentration; NCBI = National Center for Biotechnology Information; PSORTb = Prediction of Bacterial Protein Subcellular Localization; STITCH = Search Tool for Interacting Chemicals; SVM = Support Vector Machine; VICMPred = Virulence Factors Identification and Classification Using; Machine Learning Prediction; HLA = Human Leucocyte Antigen; MVs = Membrane Vesicles; ROS = Reactive Oxidative Stress.

INTRODUCTION

Dental and oral diseases are frequently neglected, particularly among residents residing in areas distant from primary healthcare facilities. One such disease is dental caries, a condition characterized by the demineralization of the enamel and dentin tissues of the teeth. (Soesilawati, 2020). According to the 2023 Indonesian Health Survey (SKI), the prevalence of caries among individuals aged 3 years and older is 33,196 cases (KEMENKES RI, 2024). The development of dental caries can be attributed to inadequate oral hygiene, the habitual consumption of high-sugar foods, and limited use of fluoride (Hamka et al., 2024). Moreover, bacteria such as the *Streptococcus mutans* group play a significant role in its etiology (Lemos et al., 2019). Residents of Central Kalimantan typically consume water sourced from peat swamp rivers, which is also utilized for bathing and washing clothes. Acidic conditions may further elevate the risk of caries due to their interference with saliva production (Nawan et al., 2023; Suratri et al., 2018).

SKI 2023 reported that 7,939 residents of Central Kalimantan opted to avoid consulting with dental health

professionals, with 37% deciding to self-medicate regardless of the chronic nature of their symptoms (KEMENKES RI, 2024). Traditional medicine became the primary choice, as it is easily accessible and consumable, adding to its appeal due to minimal perceived side effects. One study on the use of noni fruit as a source of mouthwash by Ahmad et al. in 2022 showed antibacterial effectiveness against *S. mutans* with an inhibition zone of 25.7 mm after intervention with 15% ethanol extract of *M. citrifolia L.* (Fajri Ahmad et al., 2022). However, no studies have investigated the specific virulence effects of components that target the causative bacteria. Specific virulence factors aid the pathogen colonization process at the host cellular level and interact with the immune system, which plays a role in the infection process. Virulence factors are classified into several types based on their role in disease, such as adhesion, invasion, colonization, and toxins (Denzer et al., 2020). Virulence genes in *S. mutans* can be classified into several groups based on their role, including genes involved in bacterial adhesion, extracellular polysaccharide formation, biofilm formation, sugar uptake and metabolism, acid tolerance, and genetic regulation (You, 2019).

Noni or *mengkudu* (*Morinda citrifolia L.*) is a tropical medicinal plant species known for its medicinal properties. It grows in coastal areas up to an altitude of 1,500 meters above sea level and is found in Malaysia, Indonesia, Taiwan, the Philippines, Vietnam, India, Africa, and the West Indies, particularly in Central Kalimantan, the harvest area of mengkudu, totaling 2,755 trees (Kementerian Pertanian Republik Indonesia, 2024). Overall, *Morinda citrifolia L.* extract contains pharmacological activities that act as anti-diabetic, anti-inflammatory, anti-fungal, antioxidant, anaphylactic, immunostimulant, anti-ulcerative, anti-hypertensive, and anti-bacterial agents (Ayunda et al., 2020). The secondary metabolites flavonoids and phenols are key factors in the antimicrobial properties of noni plants, with the highest potential found in the leaves and fruit (Noviana et al., 2021). Specifically, the quercetin and morin content isolated from the secondary metabolite flavonoids will be tested in this study (Ayunda et al., 2020).

The use of conventional therapies of fluoride, chlorhexidine, and synthetic antimicrobial agents, despite effectiveness, results in tooth discoloration or mucosal irritation, along with antibiotic and microbial resistance. *Morinda citrifolia L.* extract has advantages in terms of sustainability and cultural acceptance in Central Kalimantan society, which is accustomed to using local medicinal plants. Previous studies have focused on the percentage of extracts and their mixtures; it is also important to conduct research that can reveal the relationship between specific compounds in *Morinda citrifolia L.* and proteins in *S. mutans* bacteria. Bioinformatics methods can be an effective option for optimizing the target activity of noni plant component isolation to determine *S. mutans* bacteria and detect the molecular mechanism bioactivity underlying the interaction of *Morinda citrifolia L.* components with *S. mutans* bacteria. In 2024, Faisal and Arhasy revealed that bioinformatics studies had successfully identified and evaluated active components of traditional medicines with therapeutic potential for metabolic syndrome, such as *Allium sativum, Momordica charantia, Cinnamomum verum, Morinda citrifolia,* and *Curcuma longa* (Faisal & Arhasy, 2025). Bioinformatics research also serves as a complementary element alongside in vitro testing, as exemplified in the 2024 study by Wardana et al., which examined the efflux mechanism in Staphylococcus haemolyticus bacterial resistance (Wardana et al., 2024). Çolak's 2023 study also analyzed the virulence factors of Streptococcus uberis using in silico bioinformatics methods to identify chimeric multi-epitope vaccine targets. Based on the above background, the author conducted research to analyze the virulence factors of *S. mutans* strains targeted by quercetin and morin using a bioinformatics approach.

MATERIALS AND METHODS

Study area

This study used bioinformatics computational methods to analyze the bioactivity of *S. mutans* strains targeted by flavonoid components, namely quercetin and morin from *Morinda citrifolia L.* Hardware material used in this study was a set of ASUS VivoBook X415DAP_M415DA laptops with AMD Ryzen 3 3250U processors, 8.0 GB RAM, 4 CPUs ~2.6GHz, and Windows 11 operating systems, connected to the internet. The software used for data analysis was bioinformatics software, namely STITCH v5.0, VICMPred, VirulentPred, BepiPred v1.0, MHC BindPred, and PSORTb v3.0.

Inclusions and Exclusions Criteria

Inclusions

1. *S. mutans UA159* bacterial protein that interacts with quercetin and morin in STITCH v5.0.
2. FASTA *S. mutans UA159* can be found at the National Center for Biotechnology Information (NCBI).

Exclusions

1. Network disruptions and hardware damage caused by viruses or applications used.
2. The quercetin and morin components do not interact with FASTA *S. mutans UA159* entirely

Bacterial strain

The material used in this study was FASTA *S. mutans UA159*, which was downloaded from the National Center for Biotechnology Information (NCBI) website. The first complete genome sequence was that of *S. mutans strain*

UA159 in 2001, isolated from human (mammalian) dental caries disease with a sub-type ecosystem in the oral cavity (Lemos et al., 2019). The first isolation was taken from a case of active pediatric dental caries in 1982, which was non-motile and nonsporulating (Schooch, 2020).

Procedures

1. Identify interactions of *S. mutans* targeted by quercetin and morin using STITCH v5.0 software, then download FASTA from the National Center for Biotechnology Information (NCBI) database.
2. Annotate the FASTA file according to protein name and save it in different folders based on protein type.
3. The FASTA files were then used to identify the functional class, virulence properties, epitopes, and subcellular localization of *S. mutans UA159* proteins that exhibit bioactivity with quercetin and morin using the VICMPred, VirulentPred, BepiPred v1.0, MHC BindPred, and PSORTb v3.0 software.

Data analysis

Protein interaction analysis

Analysis of the interaction between the *S. mutans UA159* protein and the flavonoid component of *Morinda citrifolia L.* using the Search Tool for Interacting Chemicals (STITCH), a database of interactions between chemical compounds and proteins. STITCH can be accessed at http://stitch.embl.de/. Enter the name of the compound and select the intended bacteria on the main page. The page will display the analysis results in the form of a three-dimensional interaction structure image. Then, download the analysis results data in FASTA format from the National Center for Biotechnology Information (NCBI) database. This format will be used to predict the functional class (Szklarczyk et al., 2016).

Analysis and interpretation of the class functional

Functional class analysis using the VICMPred software by entering the previously downloaded FASTA format. The format will then be analyzed by the software into one of four available functional classes, namely virulence factors, information molecules, cellular processes, or metabolic molecules, based on their amino acid sequence. VICMPred can be accessed at https://webs.iiitd.edu.in/. Enter the FASTA data on the "SUBMISSION" page and press "Submit sequence" (Kashyap et al., 2020).

Virulence analysis and interpretation

Analysis of the virulence properties of *S. mutans UA159* protein targeted by *Morinda citrifolia L.* flavonoid components using VirulentPred software by entering the FASTA format obtained previously on the "Submit" page, selecting Dipeptide Composition Based analysis, then pressing "Submit sequence". The format will then be analyzed into one of two available groups: virulent and non-virulent. A prediction score will be provided for the virulent or non-virulent results, along with the virulence score. A more positive number indicates a higher level of virulence. Proteins identified as virulent will then be used to analyze epitopes and their subcellular locations. VirulentPred can be accessed at http://bioinfo.icgeb.res.in/virulent/submit.html (Garg & Gupta, 2008). The results of the VICMPred and VirulentPred software analyses will be presented in Table 1.

Table 1. Analysis Results of Functional Class and Virulent Factor.

Organism	Identifier	Protein interacted with Quercetin/Morin	Functional Class	Virulent factor	Virulence Score
Bacterial strain	Protein codes of virulent bacteria	List of proteins found in the analysis with the STITCH application	Results of the VICMPred analysis	List of proteins virulent	The score displayed on the website describes how strong the affinity

Epitope B-cell analysis and interpretation

Analysis of the B-cell epitope of *S. mutans UA159* protein targeted by quercetin and morin from *Morinda citrifolia L.* extract using BepiPred v1.0 software by entering the FASTA format of the protein analyzed for virulence factors on the main page and pressing "submit". The format was then analyzed to find epitope and non-epitope amino acids with scores exceeding the threshold (>0.35), which were predicted to be part of the epitope and colored yellow on the graph. BepiPred v1.0 can be accessed at http://tools.iedb.org/bcell/ (Capistrano Costa et al., 2024).

T cell cytotoxic and helper T cell Epitope analysis and interpretation

Analysis of cytotoxic T epitopes and helper proteins of *S. mutans UA159* targeted by quercetin and morin from *Morinda citrifolia L.* extract using MHC forms in MHC Binding Prediction software by entering the FASTA format of the previously analyzed virulent protein on the main page and selecting the desired allele and amino acid sequence length, MHC I uses nine amino acids, and MHC II has twelve amino acids. Then press "Submit". MHC Binding Prediction can be accessed via the pages http://tools.iedb.org/mhci/ and (ii) http://tools.iedb.org/mhcii/ (Capistrano Costa et al., 2024).

Table 2. Analysis Results of Cell T Cytotoxic and Helper T Cell Epitope.

No.	Allele	Start	End	Lenght	Peptide	Score	Percentile Rank
1.	Represents the specific HLA allele used in the prediction analysis	The starting amino acid position of the peptide	The ending amino acid position of the peptide	Number of amino acids in the peptide corresponding to the epitope size used in prediction	Amino acid sequence of the predicted epitope that potentially binds to the selected MHC molecule	Binding affinity value	Relative binding performance compared to a large dataset of random peptides

The table above explains the sequence correspondences for each predicted virulent protein peptide bond that has been tested. The column contains the expected allele used and fills in the sequence number indicating the MHC molecule to which the peptide is predicted to bind, start, and end positions, indicating the peptide's position and length. In the table, the percentile rank interpretation is more commonly used for the consensus method. The IEDB recommends 2.22, or previous versions. The prediction score is a combination of sources. The prediction results are part of IC50nM from the bacterial MIC research database. Therefore, the smaller the number, the higher the affinity. Peptides with an IC50 quantity of <50 nM are interpreted as having high affinity, <500 nM as having intermediate affinity, and <5000 nM as having low affinity (Bonsack et al., 2019).

Sub-cellular localization analysis and interpretation

Subcellular localization analysis of the *S. mutans UA159* protein targeted by quercetin and morin from *Morinda citrifolia L.* extract using PSORTb v3.0 software by selecting bacteria in the "Choose an organism type" section on the main page, selecting Gram-positive in the "Choose Gram stain" section, then entering the FASTA format of the protein previously identified as virulent. The server will then analyze and provide the results of the subcellular location of the protein based on Gram-positive bacteria, which are grouped into four subcellular locations, namely cytoplasm, cytoplasmic membrane, cell wall, or extracellular. The results of the analysis will be presented in tabular form based on the research objectives. PSORTb can be accessed via the website https://www.psort.org/psortb/ (Kashyap et al., 2020)

Table 3. Analysis Results of Virulent Protein Sub-cellular Localization.

Organism	Identifier	Functional Protein	Sub-cellular localization
Bacterial strain	Protein codes of virulent bacteria	Functional protein names	Predicted results of protein expression locations subcellular level

RESULTS AND DISCUSSION

Result of Protein Interaction

Protein interactions were analyzed using STITCH v5.0, identifying proteins from the bacteria *S. mutans UA159* that are targeted by two secondary metabolite compounds, quercetin and morin. The results showed that the two compounds interacted with ten proteins, quercetin (PknB, SMU_1806, fabZ, SMU_520, SMU_1213c, atpA, atpG, atpD, glgP, phsG) and morin (SMU_923, SMU_922, SMU_906, SMU_905, SMU_525, SMU_524, SMU_1164c, SMU_1163c, SMU_1079c, SMU_1078c). The interaction map displays varying line thicknesses and node identifiers depending on the confidence level of STITCH v5.0. Different colors also indicate the query protein and the main target source of the interactor, while white nodes display secondary interactions or the second shell of interaction. Nodes appear in small size and are identified as unknown proteins without 3D structures, while larger sizes display several predicted 3D protein structures. Line sizes with low confidence (0.150), medium confidence (0.400), high confidence (0.700), and highest confidence (0.900).

Figure 1. Interaction of quercetin targeting protein of *S. mutans*.

The interaction network displayed two interesting connections linked to each of proteins atpD, phsG, atpG, and atpA, also SMU_520 with SMU_1213c. The lines connecting atpD, atpG, and atpA have the highest confidence level with a score of 0.900 and are interconnected, meaning that the interactions of each protein influence each other even though some relationships, such as with phsG, are not strong. Meanwhile, proteins that appear to be independent in terms of their relationship with the quercetin compound do not affect interactions with other proteins.

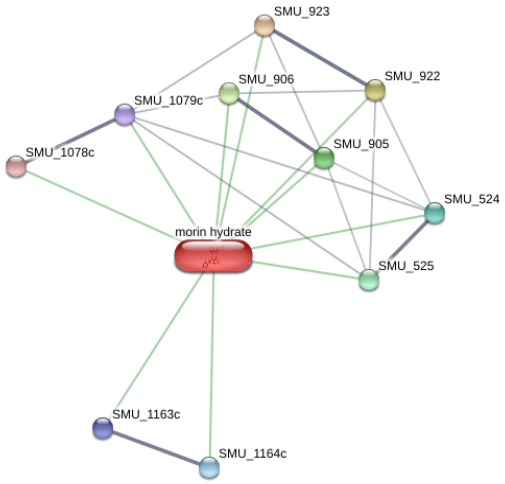

Figure 2. Morin interaction with *S. mutans UA159.*

The interaction map displayed for the interaction between morin and *S. mutans UA159* provides a more complex picture, with proteins SMU_1163c and SMU_1164c connected to each other with the highest edge confidence level and separated from the other eight proteins that form a cluster. Several proteins with closely located peptide residues have the highest confidence levels in this analysis, as they are likely to play a role in related biological functions or have covalent amino acid components.

The next key investigation after identifying bacterial proteins that interact with the target compound is functional class analysis and virulence properties. The results of the analysis show that four functional classes were found in bacteria targeted by quercetin (Table 4), namely cellular process, metabolism molecule, information molecule, and virulence factors. From the analysis of virulence properties, three virulent proteins were found, namely PknB, SMU_1806, and SMU_1213c. In addition, a hypothetical protein with an experimental chain length of 443 amino acid residues was also identified, whose biological function is not yet known with certainty. However, through this bioinformatics analysis, it is known that its biological function is likely to play a role as a metabolism molecule, even though it is not virulent. Quercetin has the potential to be a multi-target agent that influences gene regulation and expression through various mechanisms, not just one biological pathway.

Table 4. Functional class and virulent factor of *S. mutans UA159* targeted by quercetin.

Organism	Identifier	Protein interacted with Quercetin	Functional Class	Virulent factor	Virulence Score
S. mutans UA159	PknB	serine/theonine protein kinase (616 aa)	Virulence factor	virulent	0.5000
	SMU_1806	Glycosyltransferase (389 aa)	Metabolism molecule	virulent	0.8788
	fabZ	(3R)-hydroxymyristoyl-ACP dehydratase;	Metabolism molecule	Non-virulent	-0.672
	SMU_520	hypothetical protein (443 aa)	Metabolism molecule	Non-virulent	-0.456
	SMU_1213c	5'-nucleotidase	Cellular process	virulent	0.9505
	atpA	ATP synthase F0F1 subunit alpha	Cellular process	Non-virulent	-0.660
	atpG	ATP synthase F0F1 subunit gamma	Virulence factor	Non-virulent	-0.437
	atpD	ATP synthase F0F1 subunit beta	Cellular process	Non-virulent	-0.891
	glgP	glycogen phosphorylase	Information and storage	Non-virulent	-0.319
	phsG	glycogen phosphorylase	Cellular process	Non-virulent	-0.883

Whereas, in interactions with morin (Table 5), only three functional classes were found, except for virulence factors. The virulence analysis identified four virulent proteins, namely SMU_922, SMU_906, SMU_525, and SMU_1078c. The integrated results from STITCH, VICMPred, and VirulentPred show that morin is more likely to act as a metabolic modulator than a direct virulence inhibitor, but the domino effect in the regulation of proteins with virulence properties remains significant for the pathogenicity of *S. mutans*. Thus, preliminary analysis of functional classes before virulence supports the role of bacterial proteins in indirectly suppressing virulence factors to attack host tissues. Overall, proteins that interact with morin belong to the ABC transporter group, which is a large group of membrane proteins that are specific ATP-binding proteins in the cell.

Table 5. Functional class and virulent protein of *S. mutans UA159* targeted by quercetin.

Organism	Identifier	Protein interacted with Morin	Functional Class	Virulent factor	Virulence Score
S. mutans UA159	SMU_923	ABC transporter ATP-binding protein (584 aa)	Cellular Process	Non-Virulent	-0.922
	SMU_922	ABC transporter ATP-binding protein (600 aa)	Metabolism Molecule	Virulent	0.2109
	SMU_906	ABC transporter ATP-binding protein (590 aa)	Cellular process	Virulent	0.3580
	SMU_905	ABC transporter ATP-binding protein (578 aa)	Metabolism Molecule	Non-Virulent	-0.604
	SMU_525	ABC transporter ATP-binding protein (580 aa)	Metabolism Molecule	Virulent	0.248
	SMU_524	ABC transporter ATP-binding protein (587 aa)	Metabolism Molecule	Non-Virulent	-0.263
	SMU_1164c	ABC transporter ATP-binding protein (590 aa)	Cellular process	Non-Virulent	-1.085
	SMU_1163c	ABC transporter ATP-binding protein (581 aa)	Cellular process	Non-Virulent	-0.750
	SMU_1079c	ABC transporter ATP-binding protein (577 aa)	Cellular process	Non-Virulent	-0.303
	SMU_1078c	ABC transporter ATP-binding protein (581 aa)	Information and storage	Virulent	-0.5182

B-cell Epitope Analysis

The graph will appear showing two colors that differentiate the score threshold, green indicating a score >0.35 and yellow indicating a score >0.35, which is then selected as the epitope sequence. The analysis of B-cell epitopes of the seven virulent proteins of *S. mutans UA159* is as follows.

a. Analysis of B-cell epitopes of virulent proteins of *S. mutans UA159* targeted by quercetin

The three virulent proteins tested further are PknB, SMU_1806, and SMU_1213c, as shown in the figure below in sequence. There are twenty-six amino acid chains of the PknB protein that bind to B-cell antibodies. In the SMU_1806 protein test, fifteen amino acid chains were found, while the SMU_1213c protein showed thirty-two amino acid chains binding to B-cell antibodies.

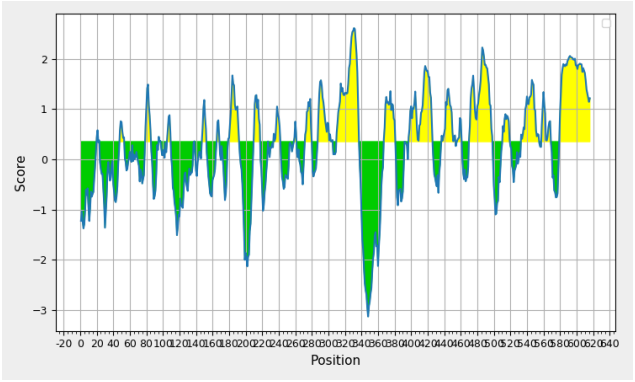

Figure 3. B-cell epitope of PknB.

The PknB protein shows several major positive peaks with yellow-colored graph indicators that exceed the threshold, indicating potential antigenic domains, yet it remains fluctuating with the positions of the main residues on the X-axis 310-336, 397-425, and 470-498 capable of being recognized by antibodies.

Table 6. PknB Protein Amino Acid Chain Binds to B-Cell Antibodies.

Start	End	Peptide	Length
20	21	RG	2
23	23	M	1
48	53	YQTDQV	6
79	85	IGEEDGQ	7
95	97	GAD	3
105	109	HAPLS	5
138	138	K	1
148	152	GTAKV	5
165	168	SLTQ	4
179	192	LSPEQARGSKATVQ	14
210	217	IPYDGDSA	8
227	227	K	1
234	242	AENKNVPQA	9
259	261	YHS	3
272	279	SLQPNRSR	8
288	305	ASDTKPLPKLEQAAANSL	18
310	336	LKNKTSNQDKVDHKSKPKTKP QPKPKK	27
367	380	PSTVSVPDVSGDKL	14
392	392	L	1
397	425	VQKIEDDNVGAGKVVRTNPSA GSKKREGS	29
437	453	FKMEDYTGQDYKDAIDN	17
456	461	NNYGVS	6
470	498	VSSDDYSGGTVIGQSPKPGKT YHPSSDKK	29
511	519	LKNSTYEEA	9
533	554	IKAYDASDYSSEISSPSSSSLV	22
558	568	SPYYGNTVSLS	11

Table 3 shows that the longest peptide chains are at residue positions 397VQKIEDDNVGAGKVVRTNPS-AGSKKREGS425 and 470VSSDDYSGGTVIGQSPKPGKTYHPSSDKK498 with an amino acid length of 29-mer. This position allows it to be an antigenic epitope that can be recognized and interact with B-cell antibodies, triggering an immune response as a form of the adaptive immune system.

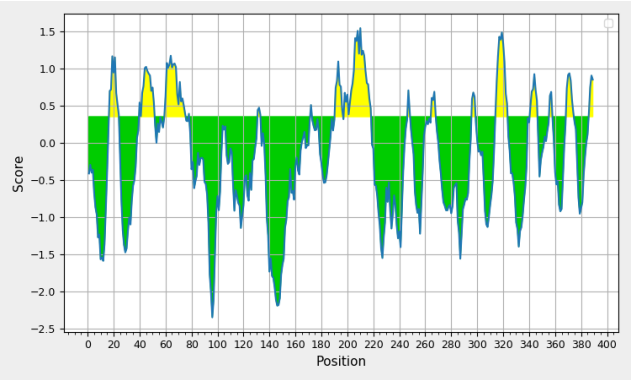

Figure 4. B-cell epitope of SMU_1806

The SMU_1806 protein shows fairly wide score fluctuations, but with a fairly stable Y-axis height at each positive epitope potential, and although more limited, there is a good level of consistency throughout the sequence. The most dominant peptide sequence in the SMU_1806 protein is at residue position 198YQYVGPSINRPVEPPFDFTPF218, with a 21-mer amino acid peptide length that biologically exhibits varying capacities for B-cell antibody binding.

Table 7. SMU_1806 Protein Amino Acid Chain Binds to B-Cell Antibodies.

Start	End	Peptide	Length
17	24	SGHTNPTL	8
40	51	INAPDWQSKIER	12
60	75	DHYPDSLSERQKKVKS	16
78	78	A	1
131	133	GKT	3
172	172	L	1
191	196	DTFDEN	6
198	218	YQYVGPSINRPVEPPFDFTPF	21
247	248	NE	2
265	268	LGTM	4
296	298	MNS	3
314	323	VGNDQPRVAQ	10
341	346	PQEIKQ	6
356	357	SY	2
369	374	QTAGGN	6

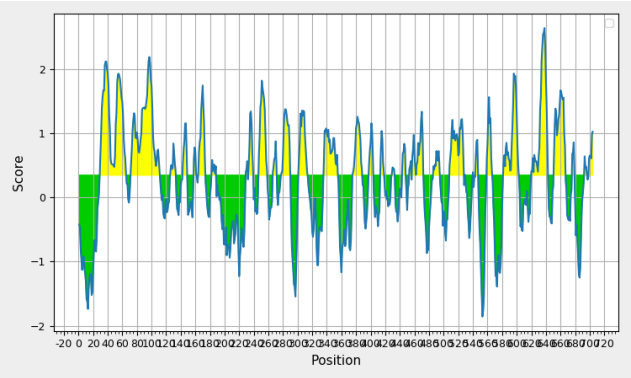

Figure 5. B-cell epitope of SMU_1213c

This third protein displayed multiple small positive peaks with shorter intervals, indicating the possibility of several scattered linear epitopes, but further verification is needed to confirm that all residues are correctly bound to B-cell antibodies. Analysis of the SMU_1213c protein shows the longest sequence potentially recognized by antibodies is 40 amino acids long, with residues 72VKSADDSKSVFEDSHSDEVSSSSASSGPKPAVNC VS-DEAT111 determining antibody binding to the epitope in sequence, independent of the tertiary structure of the antigen.

Table 8. SMU_1213c Protein Amino Acid Chain Binds to B-Cell Antibodies.

Start	End	Peptide	Length
30	65	DLTTEPSADSSTQSSSLSFSEQT ADSGQETSQVSDA	36
72	111	VKSADDSKSVFEDSHSDEVSSS SASSGPKPAVNCVSDEAT	40
126	133	EDSSNGVI	8
143	148	AESRKK	6
158	161	DAIQ	4
164	173	PITNNSKGED	10
182	188	GYDAMTV	7
229	231	VID	3
233	239	NKNIDGD	7
247	258	TTPETATKTHPR	12
266	271	TDPITE	6
278	289	QTEAQARSQGKT	12
301	313	VDTTTKEEWRGDS	13
336	355	SHTAKTQTYGNVTYNQTGSY	20
375	388	ISDQDAKTVAADPN	14
398	403	TKYKAD	6
414	418	VELNG	5
429	432	NLGN	4
443	447	QTGFS	5
453	455	AVT	3
457	472	GGGLRETIAKDKPITK	16
486	494	AQVAATGQN	9
508	527	QADDKGKSVLDENGQPLLEP	20
529	529	G	1
540	540	Y	1
544	547	SLEP	4
559	566	PETKTYQP	8
582	602	AAGGDGYTMLGGSREEGPSMD	21
620	642	INPNSRSISISSTKDSDGDGQPD	23
651	666	KATVPQKGFDSGQDKS	16
676	679	NWRA	4
693	696	PLAE	4

b. Analysis of B-cell epitopes of virulent proteins of *S. mutans UA159* targeted by morin

Based on virulent factor analysis, there are four virulent proteins targeted by the morin compound: SMU_922 with twenty-seven amino acid chains, SMU_906 identified with eighteen amino acid chains, SMU_525 with twenty-one amino acid chains, and SMU_1078c with twenty-one amino acid chains that interact with B-cell antibodies. The SMU_922 protein exhibits fluctuations in most of its protein structure, which is more hidden in terms of conformation. This allows only partial antigenic regions to be exposed to the surface,

thus limiting accessibility to antibodies compared to other proteins.

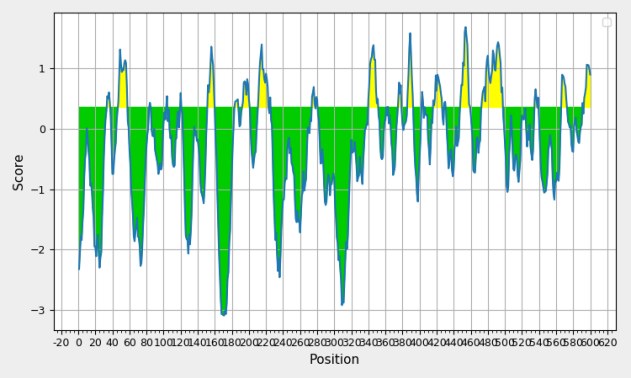

Figure 6. B-cell epitope of SMU_922

The conformational epitope complex has the potential for advanced structural involvement that needs to be analyzed further. In the SMU_922 protein, the longest peptide strand with 25-mer at residue position 473FVEEKEKGLDTEVAQGGTNFSGGQK497 has the most dominant potential in this protein to be recognized and bind to linear antibodies.

Table 9. SMU_922 Protein Amino Acid Chain Binds to B-Cell Antibodies.

Start	End	Peptide	Length
34	37	PEYM	4
47	57	KGTTASDIMDP	11
84	84	A	1
104	104	A	1
120	120	N	1
152	159	GKSDEWTG	8
183	187	QRQVQ	5
192	200	ALNSTTRES	9
211	223	NAEDYQDTKFKRE	13
225	225	K	1
274	277	VTAA	4
279	280	GA	2
340	351	YSKADNARKGEV	12
361	361	S	1
363	363	N	1
375	378	AKAG	4
386	392	STGSGKS	7
403	404	DA	2
406	406	E	1
416	426	VQDYSHDDLNN	11
429	430	GY	2
448	459	FGQSDQAPLDDA	12
473	497	FVEEKEKGLDTEVAQGGTNFS GGQK	25
535	537	AKK	3
539	539	K	1
566	572	KVVGQGT	7

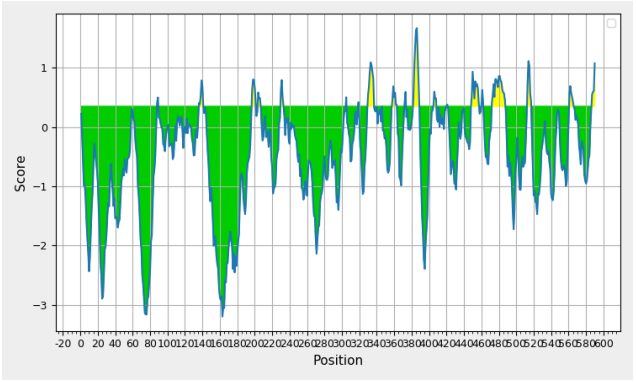

Figure 7. B-cell epitope of SMU_906

Similar to the previous protein, the SMU_906 protein displays fewer potential epitopes, indicating that the metabolism carried out by this protein plays a greater role in the internal structure of bacteria, as it shows minor accessibility to antibodies. The position of residues 472-487 may not have the highest score, but their location is more optimal and stable at the C-terminal. The major chain length of the SMU_906 (Table 10) protein was found in the epitope position of residue 472PDGYNMEVNQESNNIS487 with an amino acid length of 16-mer compared to other epitope peptide segments. This region shows the highest antibody binding probability.

Table 10. SMU_906 Protein Amino Acid_Chain Binds to B-Cell Antibodies.

Start	End	Peptide	Length
88	89	SY	2
136	141	NDVETV	6
197	201	PYFKK	5
204	206	NAL	3
230	233	EISA	4
305	305	Q	1
319	319	S	1
330	336	ETDEVNQ	7
358	363	YTEDKP	6
372	373	VK	2
382	388	GPTGAGK	7
405	408	AITV	4
420	421	EY	2
449	457	QASDEEIVE	9
460	462	KAA	3
472	487	PDGYNMEVNQESNNIS	16
513	517	TSSVD	5
561	565	IIEQG	5

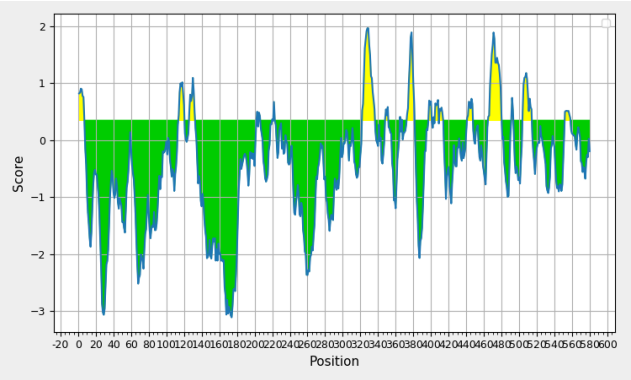

Figure 8. B-cell epitope of SMU_525

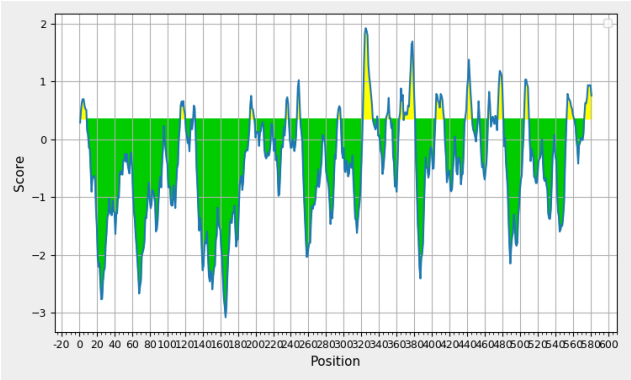

Figure 9. B-cell epitope of SMU_1078c

The SMU_525 protein displays a more dominant negative score, but this does not mean that it does not play a major role in inhibiting bacteria. It is just that the mechanism it carries is different, making it insensitive to B-cell antibodies and more hydrophobic or embedded in the protein structure. Positive spikes are more prominent at residues 332-336 and 465-480. The major chain length of the SMU_525 (Table 11) protein was found in the epitope position of residue 465KYEEPVSEGGSSFSTG480 with an amino acid length of 16-mer. This region consistently forms a peak above the positive predicted antigenicity threshold located in the C-terminal part of the protein, with an advantage over other epitope segments.

The last protein, SMU_1078c, has one dominant peak in the middle of the sequence with a score exceeding the threshold of 0.35 with high accessibility potential. The peak score at residue positions 362-380 is a segment with dominant antigenic potential. Several small linear epitopes are also scattered along the polypeptide chain. Table 5.9 shows that the longest peptide chain is at residue position 369 KVAIVGPTGAGK 380 with an amino acid length of 12-mer. This position allows it to become an antigenic epitope capable of interacting with B-cell antibodies. However, the length of the recognized peptide does not always guarantee the success of the entire epitope; it needs to be linked to biological function and accessibility according to its location in the cell.

Table 11. SMU_525 Protein Amino Acid Chain Binds to B-Cell Antibodies.

Start	End	Peptide	Length
1	7	MKNNEHQ	7
114	120	DKTPAGS	7
126	132	TNDTESI	7
203	203	N	1
205	206	SE	2
220	220	E	1
222	222	R	1
322	336	ERDYEPHQDDSDISI	15
348	351	FSYD	4
365	365	N	1
367	367	G	1
373	381	VGPTGSGKS	9
398	400	VTI	3
403	403	H	1
405	408	IRNY	4
410	413	QEEL	4
441	447	LTDADIE	7
465	480	KYEEPVSEGGSSFSTG	16
492	493	AS	2
504	514	TANIDSETEQL	11
552	558	IIESGTH	7

Table 12. SMU_1078c Protein Amino Acid Chain Binds to B-Cell Antibodies.

Start	End	Peptide	Length
2	8	KARNNKN	7
115	120	KHSSGD	6
130	131	EQ	2
194	198	TRARG	5
235	237	AKY	3
247	250	TVNP	4
293	296	KPFN	4
322	332	RDAKDDGKKEL	11
338	338	K	1
348	353	FGYDEK	6
363	367	NIPQG	5
369	380	KVAIVGPTGAGK	12
405	413	ITDYSKASY	9
438	445	GYPEASRE	8
453	454	AA	2
464	466	PQG	3
469	469	T	1
472	473	AD	2
475	481	GESLSQG	7
505	510	TSSIDT	6
553	561	IVEQGNHKD	9

Cytotoxic T cell and helper T cell Epitope analysis

A score >0 indicates that the peptide combination is more likely to elicit an immune response than <0, which indicates the opposite. Meanwhile, a percentile rank <1% indicates optimal performance when combined with a high score.

a. Cytotoxic T cell epitope of virulent protein targeted by quercetin

The analysis results show that the PknB protein possesses the highest score of 0.98 and the lowest score of 0.83, while the SMU_1806 protein has the highest score of 0.91 with the lowest score of 0.76, and the SMU_1213c protein has the highest score of 0.93 and the lowest score of 0.60. PknB showed the best performance compared to other virulent proteins targeted by quercetin, with the highest score of 0,98 supported by an affinity percentile rank of 0,00. The peptide with the highest score has a prediction value of 0.98 and a percentile rank of 0.00, placing it as the peptide with the strongest bond among all PknB protein candidates in Table 13 because it can produce results of <1%. Overall, the minimum absolute value was achieved by five major peptide chains with a percentile rank of 0.00.

Table 13. PknB Cytotoxic T Cell Epitope.

No.	Allele	Start	End	Lenght	Peptide	Score	Percentile Rank
1	HLA-A*11:01	381	389	9	STAKMIIRK	0.98	0.00
2	HLA-A*11:01	489	497	9	KTYHPSSDK	0.95	0.00
3	HLA-A*11:01	412	420	9	RTNPSAGSK	0.90	0.00
4	HLA-A*11:01	122	130	9	SAMTLAHQK	0.89	0.00
5	HLA-A*11:01	494	502	9	SSDKKITLK	0.83	0.00

The analysis of cytotoxic T cell epitope predictions for the SMU_1806 protein in Table 14 shows varying binding affinities with the highest score of 0.91, supported by a percentile rank of 0.00, indicating the most dominant predictive position among all epitope candidates. However, among them, the lowest score of 0.76, with a percentile rank of 0.00, is better than the peptide with a score of 0.78 and a percentile rank of 0.01, indicating an overlap in the prediction values of several candidates. This still indicates that the SMU_1806 protein contains the potential for more than one peptide.

Table 14. SMU_1806 Cytotoxic T Cell Epitope.

No.	Allele	Start	End	Lenght	Peptide	Score	Percentile Rank
1	HLA-A*11:01	324	332	9	QVADLHLGK	0.91	0.00
2	HLA-A*11:01	345	353	9	KQAAHTILK	0.84	0.00
3	HLA-A*11:01	140	148	9	SIFRFTFLR	0.81	0,00
4	HLA-A*11:01	380	388	9	TIIKDLQTK	0.78	0.01
5	HLA-A*11:01	350	358	9	TILKDSSYK	0.76	0.00

Table 15 shows that the analysis of the SMU_1213c protein has a peptide with the highest score of 0.93 and the most optimal percentile rank of 0.00, indicating the most dominant predictive position among all candidates because no other peptides with similar values were found, confirming that the RSISISSTK peptide is the only candidate with the highest affinity.

Table 15. SMU_1213c Cytotoxic T Cell Epitope.

No.	Allele	Start	End	Lenght	Peptide	Score	Percentile Rank
1	HLA-A*11:01	625	633	9	RSISISSTK	0.93	0.00
2	HLA-A*11:01	65	73	9	AISSVAAVK	0.80	0.01
3	HLA-A*11:01	246	254	9	VTTPETATK	0.79	0.01
4	HLA-A*11:01	603	611	9	SIFTDYLSR	0.71	0.01
5	HLA-A*11:01	433	441	9	AVADALLDY	0.62	0.01

b. Cytotoxic T cell epitope Virulent protein targeted by morin

The analysis results show that the highest score of 0.92 and the lowest score of 0.77 are possessed by the SMU_922 protein, while the SMU_906 protein has a highest score of 0.79 and a lowest score of 0.69, the SMU_525 protein has a highest score of 0.94 and a lowest score of 0.52, while the highest score of 0.98 and the lowest score of 0.80 were obtained by SMU_1078c as the candidate protein with the best performance

because it had a percentile rank of 0.00 and the highest score compared to other virulent proteins targeted by morin.

The results of the analysis of Table 16 on the SMU_922 protein show the three highest peptides with the most optimal percentile rank of 0.00, but the highest affinity score is held by ALNSSVHFK with a value of 0.92, describing it as the best candidate based on the prediction parameter capable of acquiring 80% of the immune response from many alleles.

Table 16. SMU_922 Cytotoxic T Cell Epitope.

No.	Allele	Start	End	Lenght	Peptide	Score	Percentile Rank
1	HLA-A*11:01	330	338	9	ALNSSVHFK	0.92	0.00
2	HLA-A*11:01	81	89	9	RTAASFTTR	0.86	0.00
3	HLA-A*11:01	566	574	9	KVVGQGTHK	0.84	0.00
4	HLA-A*11:01	501	509	9	AIARALARK	0.78	0.01
5	HLA-A*11:01	334	342	9	SVHFKEYSK	0.77	0.01

Table 17 shows the results of the analysis of the SMU_906 protein with the highest score of 0.79 for the first two levels and an identical percentile rank of 0.01 for the five peptide chains produced, even though the score gradually decreased.

Table 17. SMU_906 Cytotoxic T Cell Epitope.

No.	Allele	Start	End	Lenght	Peptide	Score	Percentile Rank
1	HLA-A*11:01	186	194	9	FSSHFILRK	0.79	0.01
2	HLA-A*11:01	535	543	9	RTSFVIAHR	0.79	0.01
3	HLA-A*11:01	20	28	9	SLFLAIFLK	0.74	0.01
4	HLA-A*11:01	380	388	9	VVGPTGAGK	0.71	0.01
5	HLA-A*11:01	113	121	9	KINKIPVSY	0.69	0.01

The peptides with the highest scores (Table 18) of 0.94 and 0.92 have a percentile rank of 0.00, representing the most optimal affinity among all analyzed epitope candidates. In addition, peptides with scores of 0.78 and a percentile rank of 0.01 were also found, as well as two other peptides with scores of 0.58 and 0.52, each with a percentile rank of 0.02. This distribution illustrates that the two main peptides occupy the highest and most dominant prediction positions, while the other candidates show a gradual decline in affinity values and percentile levels.

Table 18. SMU_525 Cytotoxic T Cell Epitope.

No.	Allele	Start	End	Lenght	Peptide	Score	Percentile Rank
1	HLA-A*11:01	556	564	9	GTHEELLAK	0.94	0.00
2	HLA-A*11:01	355	363	9	QILDHISFK	0.92	0.00
3	HLA-A*11:01	315	323	9	RVFDLIDER	0.78	0.01
4	HLA-A*11:01	229	237	9	AINEEHFHY	0.58	0.02
5	HLA-A*11:01	9	17	9	HVFWRLMSY	0.52	0.02

Table 19 shows the results of the analysis of the SMU_1078c protein with an optimal percentile rank of 0.00, belonging to four peptide chains with scores of 0.98, 0.96, 0.88, and 0.83 among all epitopes analyzed. Meanwhile, peptides with a score of 0.80 only show a percentile rank of 0.01, indicating a decrease in relative affinity.

Table 19. SMU_525 Cytotoxic T Cell Epitope.

No.	Allele	Start	End	Lenght	Peptide	Score	Percentile Rank
1	HLA-A*11:01	556	564	9	GTHEELLAK	0.94	0.00
2	HLA-A*11:01	355	363	9	QILDHISFK	0.92	0.00
3	HLA-A*11:01	315	323	9	RVFDLIDER	0.78	0.01
4	HLA-A*11:01	229	237	9	AINEEHFHY	0.58	0.02
5	HLA-A*11:01	9	17	9	HVFWRLMSY	0.52	0.02

c. Helper T cell epitope Virulent protein targeted by quercetin

The results of T-helper cell epitope prediction analysis with MHC-II Binding Prediction for several virulent proteins that interact with quercetin show a wide range of affinity levels. The PknB protein had the highest score of 5.83 and the lowest of 2.99, while the SMU_1806 protein showed the highest score of 4.29 and the lowest of 1.90. The SMU_1213c protein showed the highest score of 2.45 and the lowest of 1.76. In general, the positive score range indicates that the peptide combinations in the three proteins have the potential to elicit an immune response through T helper cell activation, with higher values indicating stronger affinity and MHC-II binding potential. Based on the analysis results, PknB showed the most optimal performance, supported by the highest score with a percentile rank of 0.00.

Analysis of Table 20 shows that the peptide with the highest score of 5.83 has the highest percentile rank of 0.00, followed by a gradual decrease in score and percentile rank to 0.01 and 0.02. This indicates that in the PknB protein, there is only one peptide row that has the best affinity level.

Table 20. PknB helper T Cell Epitope.

No.	Allele	Start	End	Lenght	Peptide	Score	Percentile Rank
1	HLA-DRB1*04:01	99	110	12	KKYIQDHAPLSN	5,83	0,00
2	HLA-DRB1*04:01	539	550	12	SDYSSEISSPSS	4,33	0,01
3	HLA-DRB1*04:01	98	109	12	LKKYIQDHAPLS	3,93	0,01
4	HLA-DRB1*04:01	100	111	12	KYIQDHAPLSNA	3,61	0,01
5	HLA-DRB1*04:01	39	50	12	VAIKVLRTNYQT	2,99	0,02

There are unique results found in Table 21 the overlap of the SMU_1806 protein peptide chain score with the highest score of 4.29 but a percentile rank of 0.01. In addition, the second-highest score of 2.70 achieved a percentile rank of 0.00, meaning that the affinity is not as high as the first, but its strength may be superior. This is followed by a gradual decrease in scores with subsequent percentile ranks of 0.04 and 0.05.

Table 21. SMU_1806 helper T Cell Epitope.

No.	Allele	Start	End	Lenght	Peptide	Score	Percentile Rank
1	HLA-DRB1*04:01	37	48	12	VTYINAPDWQSK	4,29	0,01
2	HLA-DRB1*04:01	184	195	12	REFQIDADTFDE	2,70	0,00
3	HLA-DRB1*04:01	36	47	12	NVTYINAPDWQS	2,31	0,04
4	HLA-DRB1*04:01	248	259	12	EPYSIIISLGNR	2,23	0,04
5	HLA-DRB1*04:01	157	168	12	RTFQLAYDDLAK	1,90	0,05

The results of the analysis in Table 22 show that the percentile rank is not as optimal as before, even though it ranks among the top five peptides. The highest score is 2.45 with a percentile rank of 0.03. Although it is not ≤0.01, it can still be classified as strong in affinity, even though it is not optimal. The lowest percentile rank of 0.05 is also accompanied by a lower score of 1.76.

Table 22. SMU_1213c helper T Cell Epitope.

No.	Allele	Start	End	Lenght	Peptide	Score	Percentile Rank
1	HLA-DRB1*04:01	642	653	12	DYLQLIADNKAT	2,45	0,03
2	HLA-DRB1*04:01	372	383	12	NALISDQDAKTV	2,23	0,04
3	HLA-DRB1*04:01	675	686	12	KNWRADQSLLIS	2,20	0,04
4	HLA-DRB1*04:01	122	133	12	GRFLEDSSNGVI	2,02	0,04
5	HLA-DRB1*04:01	398	409	12	TKYKADSSTILI	1,76	0,05

d. Helper T cell epitope Virulent protein targeted by morin

The results of T helper cell epitope prediction analysis using MHC-II Binding Prediction on several virulent proteins that interact with morin compounds show a wide range of affinity levels. Protein SMU_906 has the highest score of 6.05 and the lowest of 4.19, occupying the most optimal position in MHC-II affinity prediction compared to other proteins. Furthermore, the SMU_922 protein showed the highest score of 5.45 and the lowest of 2.20, while the SMU_1078c protein showed the highest score of 4.24 and the lowest of 2.65. The SMU_525 protein produced the highest score of 1.80 and the lowest of 0.71, with a relatively lower range of values compared to other candidates. In general, the entire range of positive scores indicates that all four proteins have the potential to trigger T helper cell activation, with SMU_906 being the most dominant candidate due to its highest affinity score in the overall analysis.

The results of the analysis in Table 23 show that the SMU_922 protein has the potential to bind MHC-II based on the best score and percentile rank variations of 5.45 and 4.72, respectively, with an identical percentile rank of 0.00, indicating that both have a high potential to trigger T helper cell activation. The subsequent peptides show a score of 3.83 with a percentile rank of 0.01, which is still considered good in the top 1%. Meanwhile, the scores of 2.93 and 2.20 show a gradual decrease in affinity strength, but remain significant at 0.03-0.04.

Table 23. SMU_922 helper T Cell Epitope.

No.	Allele	Start	End	Lenght	Peptide	Score	Percentile Rank
1	HLA-A*11:01	356	367	12	VSFRYSKNSRAV	5,45	0,00
2	HLA-A*11:01	355	366	12	DVSFRYSKNSRA	4,72	0,00
3	HLA-A*11:01	75	86	12	VGFLASRTAASF	3,83	0,01
4	HLA-A*11:01	357	368	12	SFRYSKNSRAVI	2,93	0,03
5	HLA-A*11:01	522	533	12	LDYKTDRILRND	2,20	0,04

Analysis of Table 24 shows that the SMU_906 protein provides the best affinity level for peptide chains with a score of 6.05 and a percentile rank of 0.00, which is also shared by scores of 5.18 and 5.53, which are in third place because their percentile ranks were rounded up to higher values. Meanwhile, the last two scores are 4.27 and 4.19 with a percentile rank of 0.01.

Table 24. SMU_906 helper T Cell Epitope.

No.	Allele	Start	End	Lenght	Peptide	Score	Percentile Rank
1	HLA-A*11:01	473	484	12	DGYNMEVNQESN	6,05	0,00
2	HLA-A*11:01	472	483	12	PDGYNMEVNQES	5,18	0,00
3	HLA-A*11:01	197	208	12	PYFKKQANALGD	5,53	0,00
4	HLA-A*11:01	474	485	12	GYNMEVNQESNN	4,27	0,01
5	HLA-A*11:01	196	207	12	QPYFKKQANALG	4,19	0,01

Analysis of the SMU_525 protein in Table 25 shows suboptimal results compared to other protein tests. as seen from the highest percentile rank of only 0.05 occupied by scores of 1.80, 0.98, and 0.89, with the rest decreasing and showing that it is not a potential peptide target with a low score of 0.08-0.09, which exceeds the top 1% score.

Table 25. SMU_525 helper T Cell Epitope.

No.	Allele	Start	End	Lenght	Peptide	Score	Percentile Rank
1	HLA-A*11:01	423	434	12	EPFLYHGTIKSN	1,80	0,05
2	HLA-A*11:01	422	433	12	QEPFLYHGTIKS	0,98	0,05
3	HLA-A*11:01	188	199	12	KVIAKTRSLLSD	0,89	0,05
4	HLA-A*11:01	51	62	12	DHFLTHFNQTAA	0,79	0,08
5	HLA-A*11:01	195	206	12	SLLSDINTNLSE	0,71	0,09

The results of the analysis on the SMU_1078c protein are shown in Table 26, with the highest score of 4.24 and a percentile rank of 0.01, followed by 3.68. Meanwhile, scores of 2.92, 2.88, and 2.65 obtained a percentile rank of 0.03, which is still considered good, but their performance has declined, leaving only two peptide chains with the best scores that have an optimal chance of interacting with T helper cells.

Table 26. SMU_1078c helper T Cell Epitope.

No.	Allele	Start	End	Lenght	Peptide	Score	Percentile Rank
1	HLA-A*11:01	241	252	12	AIFYSSTVNPAT	4,24	0,01
2	HLA-A*11:01	567	578	12	GVYYQMQTAQDS	3,68	0,01
3	HLA-A*11:01	240	251	12	GAIFYSSTVNPA	2,92	0,03
4	HLA-A*11:01	566	577	12	KGVYYQMQTAQD	2,88	0,03
5	HLA-A*11:01	242	253	12	IFYSSTVNPATR	2,65	0,03

Sub-cellular localization analysis and interpretation

The subcellular localization was observed for each virulence protein targeted by the two compounds quercetin and morin using PSORTB v3.0 software. Three virulence proteins targeted by quercetin produced different localizations, including the cytoplasmic membrane localization of PknB, SMU_1806 in the cytoplasm, and SMU_1213c in the cell wall.

Table 27. Sub-cellular Localization of *S. mutans UA159* Protein Targeted by Quercetin.

Organism	Identifier	Functional Protein	Sub-cellular Localization
S. mutans UA159	PknB	Serine/theonine protein kinase (616 aa)	*Cytoplasmic membrane*
	SMU_1806	Glycosyltransferase (389 aa)	*Cytoplasmic*
	SMU_1213c	5'-nucleotidase	*Cell wall*

Whereas the four proteins targeted by morin all result in subcellular locations in the cytoplasmic membrane.

Table 28. Sub-cellular Localization of *S. mutans UA159* Protein Targeted by Morin.

Organism	Identifier	Functional Protein	Sub-cellular Localization
S. mutans UA159	SMU_922	ABC transporter ATP-binding protein (600 aa)	*Cytoplasmic membrane*
	SMU_906	ABC transporter ATP-binding protein (590 aa)	*Cytoplasmic membrane*
	SMU_525	ABC transporter ATP-binding protein (580 aa)	*Cytoplasmic membrane*
	SMU_1078c	ABC transporter ATP-binding protein (581 aa)	*Cytoplasmic membrane*

Discussion

Research on the bioactivity analysis of *S. mutans UA159* bacteria targeted by quercetin and morin compounds using a bioinformatics approach has been conducted, starting with protein interaction analysis using STITCH v.5.0 software. The first analysis targeted by quercetin produced ten interacting proteins and resulted in cross-interactions between several proteins, such as the atpD, phsG, atpG, and atpA proteins, as well as SMU_520 and SMU_1213c. Meanwhile, in the interaction between morin and *S. mutans UA159* bacteria, the SMU_1163c and SMU_1164c proteins are connected and separated from the other eight proteins. This situation can occur due to similarities in amino acid sequences, similar functions, or shared biological interactions that support each other's bacterial cell performance (Nawan et al., 2025). Several proteins resulting from interactions in the form of transporters play an important role in delivering

antimicrobial effectors and destroying the resistance of gram-positive bacteria, such as *S. mutans UA159*, because gram-positive bacteria have a dense, waxy, and hydrophobic extracellular protective layer that makes it difficult to enter and penetrate mycomembranes (Green & Mecsas, 2016). The binding of ABC Transporters with ATP binding enhances the regulation of bacterial defenses against environmental stress or antimicrobials. However, their role is also considered vital in the development of antimicrobial therapeutic agents by promoting antibody stimulation, mimicking substrates, and becoming vaccine targets. SMU_1806, identified as glucosyltransferase (GFTs), plays a role in the formation of *S. mutans* bacterial biofilms. The action of GFTs results in the synthesis of adhesive glucan from sucrose, causing bacterial cells to bind to the surface of teeth. The ability of quercetin to interact with SMU_1806 provides insight into the compound's potential to inhibit the biofilm adhesion process and the mechanism of bacterial bond stability inhibition. A similar process was also found in previous studies targeting the GFTs domain of *S. mutans* with oolong tea (Matsumoto-Nakano, 2018).

The amino acid chain of proteins substantially contributes as a source of energy generation, depending on the metabolic status of biota (Kandasamy et al., 2018). Both SMU_1163c and SMU_1164c proteins have the same “cellular process” role, so this mechanism can distinguish them from other protein groups, in addition to their same role as ABC Transporters of all proteins in the second interaction. This cellular process plays a role in cell division and signal transduction. On the other hand, metabolism molecules as a functional class in several proteins indicate that energy production, transport, and metabolism of carbohydrates, amino acids, nucleotides, and lipids in *S. mutans UA159* bacteria are regulated by the seven proteins obtained from two bacterial interactions targeted by quercetin and morin compounds (Zhang et al., 2024). Proteins identified as belonging to the “information and storage” functional class, namely glycogen phosphorylase and ABC transporter ATP-binding protein (581 aa), play a role in protein expression memory, starting from the development of DNA and RNA sequences for cell signaling and bacterial gene transcription (Lyon, 2015). “Virulence factors” identified by functional class using VicmPred are based on biological function, so they are still predictive, such as serine/threonine protein kinase (616 aa) and ATP synthase F0F1 gamma subunit. The benchmarks in this analysis are based on adhesion, toxins, and hemolytic molecules. Meanwhile, the virulence analysis results show the empirical ability of a protein to contribute to the pathogenesis mechanism through motility performance, adherence, and the ability to form biofilms to survive in diverse environments and resist antibiotics (Kumkar et al., 2022).

The seven proteins that were subsequently identified as having virulence properties after analysis with VirulentPred consisted of serine/threonine protein kinase, glycosyltransferase, and 5'-nucleotide targeted by quercetin, and ABC Transporter ATP-binding protein targeted by morin. The best score in this analysis was 0.950 for 5'-nucleotide. Serine/threonine protein kinase (STPK) supports cell growth and division, maintains antibiotic persistence, virulence, and bacterial infection in the host. ABC Transporters have two important roles as importers and exporters that contribute to the virulence and pathogenicity of bacteria that have been studied in E. coli, S. aureus, and S. pneumoniae (Nagarajan et al., 2022). 5'-Nucleotides function to break down nucleotides into nucleosides by releasing phosphate groups at the 5' position. Additionally, it can produce adenosine, which suppresses the host's immune response, leading to immune environment manipulation, as seen in S. aureus through metabolic and immune-evasive strategies. If mutations and penetration of other compounds capable of binding to 5'-nucleotides occur, the potential for antimicrobials and vaccines may be reversed because this can weaken the immune cells of bacteria, thereby thwarting the virulence of bacteria.

The subcellular locations of seven virulence proteins were found in three locations, namely the cytoplasmic membrane, cytoplasm, and cell wall. Each location determines the role and mechanism performed by the protein in supporting a bacterium's virulence strategy. The cytoplasmic membrane contains STPK or PknB and the ABC Transporter ATP Binding. In terms of process, PknB is essential in the defense and modulation of cell shape, growth, and bacterial virulence, especially the bifunctional ability of the PBP PonA1 enzyme produced by PknB through phosphorylation in the cytoplasm, which can regulate the length of a cell. When quercetin targets PknB and causes protein depletion, this can affect the phosphorylation process, which influences other proteins involved in cell wall or peptidoglycan synthesis and transcription control due to stress exposure from nutrients or osmotic pressure (Nagarajan et al., 2022). ABC Transporters themselves are reported to contribute to MDR by exporting antibiotics out of the cytoplasm, but on the other hand, they also have the potential to counteract MDR through mutation and substrate mimicry. Its performance as an importer operating on the cytoplasmic membrane in Gram-positive bacteria enables them to bind directly to membrane-bound lipoproteins and play a role in acquiring essential nutrients even when there are significant changes in the host environment, thereby facilitating the colonization of pathogenic bacteria. Meanwhile, ABC exporters play a role in transporting glycans across the inner membrane to the outside of the membrane. Through this mechanism, morin is able to target ABC Transporters, thereby potentially eliminating key determinants of bacterial virulence (Akhtar & Turner, 2022). According to the analysis results, 5'-nucleotides in the cell wall are capable of carrying out an immunoevasive mechanism. The study found that Gram-positive bacterial 5'-nucleotides increase the concentration of extracellular

immunosuppressants and help bacteria survive in the host body during infection. If they are able to maintain their position in the cell wall, they have promising characteristics for targeting proteins for vaccine production (Akhtar & Turner, 2022). Meanwhile, intracellularly, if 5'-nucleotides are successfully targeted by quercetin, it provides a pathway for the compound to disrupt the defense and repair of DNA and RNA synthesis. Glycosyltransferase is the only virulence protein identified. According to the results of the analysis, 5'-nucleotides in the cell wall are capable of carrying out an immunoevasive mechanism. In the study, it was found that Gram-positive bacterial 5'-nucleotides increase the concentration of extracellular immunosuppressants and help bacteria survive in the host body during infection. Furthermore, if they can maintain their position in the cell wall, they have promising characteristics for targeting proteins for vaccine production. Bacteria release membrane vesicles (MVs) that play a role in diverse biological processes, including intercellular communication that affects immunomodulatory activity. Failure or disruption of the cell wall determines the outcome of cytoplasmic MVs (Nagasawa et al., 2025). When both subcellular locations can be targeted by compounds, this can trigger the death of *S. mutans* cells and their invasion, because biofilm formation depends on the integrity of the cell wall and cytoplasm.

Further analysis to determine linear B-cell epitopes in proteins with positive virulence properties in *S. mutans* bacteria using BepiPred v1.0, based on the sequence length of several proteins exceeding 250 residues, with a more stable prediction accuracy for large proteins and complex domain structures. This test was conducted to identify antigenic regions that are potentially recognized by the immune system, allowing for a better understanding of the functional targets of bioactive molecular interactions. Epitopes from bacterial coat proteins are recognized by B-cell surface immunoglobulins, causing bacterial cells to be internalized and degraded. Peptides from bacterial proteins, including internal ones, are presented on the surface of B cells bound to MHC class II molecules (Janeway CA Jr et al., 2001). Of the seven proteins targeted by two different compounds in this study, the predicted epitope region graph showed yellow peaks exceeding the threshold of 0.35 as the most prominent image of residues playing a role in immunological recognition. The binding of the secondary metabolite compounds quercetin and morin can disrupt the biological function of proteins in the process of biofilm formation or adhesion to tooth surfaces. Quercetin has broad-spectrum antibacterial properties against both gram-positive and gram-negative bacteria. A study revealed that *S. mutans* growth was inhibited at a MIC concentration of 500 μg/mL on coated dentin surfaces, thereby inhibiting the adhesion and biofilm formation processes. Morin itself acts to block the pathway of molecules between the intracellular and extracellular spaces, which is usually caused by the interaction of lipid and membrane protein components, thereby inhibiting the exchange of ions (Na+, K+, H+) and nutrient molecules. Peptidoglycan cross-links are disrupted because the balance of the cell wall structure is damaged. In *S. mutans*, as a gram-positive bacterium, this reduces its ability to adhere to tooth surfaces and causes leakage of cytoplasmic components (Yaneva et al., 2022). Non-epitope results indicated by a threshold value of less than 0.35 and peptide residue lenght >30 have the potential to be conformational peptide components consisting of non-adjacent residues in the primary protein sequence but united by a structure that is partially linear and discontinuous. Accurate prediction is highly dependent on the 3D structure of the antigen (Galanis et al., 2021).

Cytotoxic T cells, part of the MHC I interaction analysis, showed that seven *S. mutans* proteins had strong binding to the individual class HLA-A*11:01, the most prevalent allele in Southeast Asia. In general, humans express the HLA-A, HLA-B, and HLA-C in the HLA molecule genes (Hamidinia et al., 2025; Tadros et al., 2025). The highest points in each of the top five ranking tables for each protein interacting with quercetin and morin compounds indicate that there is a link between epitopes and proteins with individual classes as an important indication for the development of T cell-based immunological therapeutic agents that can adapt to pathogen-specific immunity and promote B-cell epitope interactions. The better the binding performance, the smaller the percentile rank, and conversely, the higher the score when producing a dominant bond with the MHC I HLA-A*11:01 allele.

Helper T cells bound to peptide chains were identified by MHC II analysis, resulting in peptide chains from *S. mutans* proteins that were able to bind fully with scores and percentile ranks. Complex identified by helper T cell helps activate B-cell to enhance production of antibodies against coat protein. The individual allele classes used were HLA-DRB1*04:01 and HLA-DRB1, obtained from peripheral blood DNA samples using the polymerase chain reaction (PCR) method and amplification with human-specific sequence primers (Tadros et al., 2025). These alleles act as antigenic peptide molecules against CD4+ cells to trigger the downstream inflammatory process. The selection of amino acid residue 12 based on the range of 11-13 shows a stronger association than other amino acid positions (Raychaudhuri, 2010). HLA-DRB1*04:01 can help B lymphocytes specifically, and its pathway is shortened through the endoplasmic reticulum to the lysosome, resulting in a better antigenic peptide association process. The prominent score found in the T helper cell binding analysis helps us understand that the compound has the opportunity to stimulate an immune response through bacterial proteins, thereby inhibiting invasion.

The contribution of morin metabolites as anti-inflammatory and antioxidant agents is an important factor in enabling the host to respond to the presence of foreign substances that attack the body. Research by Sales et al. in 2025 revealed antioxidant activity with parameters of reduced ROS formation by neutrophils, which causes the death and degradation of pathogens as an essential innate immune response. Their study results show the important role of morin in inhibiting ROS caused by bacteria relevant to periodontitis, such as *F. Nucleatum and P. gingivalis* (Sales et al., 2025). As an additional advantage as an antimicrobial, it was concluded that it is involved in bacterial aggregation activity, the induction of oxidative stress in bacteria, and interactions with lipids from the phospholipid bilayer structure of bacterial membranes. The increased interaction due to the induction of morin compounds enhances membrane permeability, which affects the thickness of the structure that indirectly controls the distribution and function of membrane proteins, so that toxins can settle and important substances for bacteria are inhibited, causing cell integrity to decline and leading to bacterial mortality. The beneficial barrier on the host side is supported by morin by inhibiting bacterial toxins and nucleic acid synthesis, triggering disruption in the processes of gene replication and transcription (Górniak et al., 2019). Morin is special because of its chemical structure, known for the number of hydroxyl groups it contains, which enable morin to interact strongly with cell membranes and increase the compound's ability to penetrate the strong and dense layers of bacterial biofilms (Salehi et al., 2020).

The benefits of morin are more effective when combined with morin compounds that have antiparasitic properties correlated with mitochondrial dysfunction and inhibition of important enzymes and molecules such as heat shock proteins, acetylcholinesterase, DNA topoisomerases, and kinases. The death of parasites or other foreign objects caused by quercetin through apoptosis is evidenced by increased ROS and DNA degradation. The indirect biological effect of quercetin is the production of nitric oxide and cytokines that can simultaneously activate B-cells. Its ability as an anti-cancer agent is also considered through its signal transduction activity as a modulator to prevent, inhibit, and even reverse carcinogenesis, leading to increased apoptosis, cell migration, differentiation and proliferation, oxidative balance, and inflammation. Its antioxidant performance is also related to its anti-cancer potential through the inhibition of enzymes that contribute to carcinogenic activity (Salehi et al., 2020).

CONCLUSIONS

Based on research conducted to analyze the virulence factors of *Streptococcus mutans* targeted by quercetin and morin through a bioinformatics approach, the following conclusions were drawn:

1. Molecular bioactivity against *S. mutans* proteins after targeting with quercetin and morin was analyzed using STITCH v5.0, marked by a map of the relationship between proteins and selected compounds, namely quercetin (PknB, SMU_1806, fabZ, SMU_520, SMU_1213c, atpA, atpG, atpD, glgP, phsG) and morin (SMU_923, SMU_922, SMU_906, SMU_905, SMU_525, SMU_524, SMU_1164c, SMU_1163c, SMU_1079c, SMU_1078c). The identification indicates cross-interactions between proteins as an indication of linear amino acid sequences or functional classes and subcellular locations.
2. The results of virulence factor analysis using VirulentPred identified the following seven proteins: PknB, SMU_1806, SMU_1213c, SMU_922, SMU_906, SMU_525, and SMU_1078c. This is indicated by a score >0, with a higher score indicating better protein performance as a virulence factor.
3. The biological profile factors found in this study are:
   - The functional classes of each of the ten proteins identified as quercetin targets consist of four functional classes, namely cellular process, metabolism molecule, information molecule, and virulence factors. Meanwhile, proteins targeted by morin do not have virulence factors, although potential virulence factors were found.
   - Analysis of B-cell epitopes with seven virulent proteins using BepiPred v1.0 showed prominent B-cell epitope locations against *S. mutans*, as indicated by a graph exceeding the threshold of 0.35 in yellow.
   - Cytotoxic T cell and helper T cell epitopes were analyzed through MHC I and MHC II Binding Protein to examine the development of intercellular relationships, revealing peptide chains that could bind fully with sequences based on the displayed rankings.
   - The subcellular locations of the seven proteins are quite diverse, ranging from the cell wall, cytoplasmic membrane, and cytoplasm. The proteins collectively protect the bacteria from the host's extreme environment; however, disruption at any one location can lead to cell death, particularly disruption of the cell wall.

Acknowledgements: The authors are grateful to academic mentors from the Department of Microbiology and the Department of Pharmacology, Faculty of Medicine, Universitas Palangka Raya, for their guidance and support throughout the development and preparation of this manuscript.

Authors' Contributions: Saputri A.E., Praja R.K., dan Frethernety A. conceived the study and undertook the

literature review. Saputri A.E., independently and in collaboration with Praja R.K., executed the bioinformatic analysis. Turnip O.N. dan Ysrafil reviewed the manuscript and provided essential revisions prior to approval of the final version for publication.

Competing Interests: The authors declare that there are no competing interests.

Funding: The authors declare no external funding for the study.

REFERENCES

Akhtar, A. A., & Turner, D. P. (2022). The role of bacterial ATP-binding cassette (ABC) transporters in pathogenesis and virulence: Therapeutic and vaccine potential. *Microbial Pathogenesis*, *171*. https://doi.org/10.1016/j.micpath.2022.105734

Ayunda, M. N., Zulharmita, Azizah, Z., & Rivai, H. (2020). Review of Phytochemical and Pharmacological Activities of Noni (*Morinda citrifolia L.*). *Scholars Academic Journal of Pharmacy*, *9*(12), 340–346. https://doi.org/10.36347/sajp.2020.v09i12.003

Bonsack, M., Hoppe, S., Winter, J., Tichy, D., Zeller, C., Küpper, M. D., Schitter, E. C., Blatnik, R., & Riemer, A. B. (2019). Performance Evaluation of MHC Class-I Binding Prediction Tools Based on an Experimentally Validated MHC–Peptide Binding Data Set. *Cancer Immunology Research*, *7*(5), 719–736. https://doi.org/10.1158/2326-6066.CIR-18-0584

Capistrano Costa, N. T., de Souza Pereira, A. M., Silva, C. C., Souza, E. de O., de Oliveira, B. C., Ferreira, L. F. G. R., Hernandes, M. Z., & Pereira, V. R. A. (2024). Exploring Bioinformatics Solutions for Improved Leishmaniasis Diagnostic Tools: A Review. *Molecules*, *29*(22), 5259. https://doi.org/10.3390/molecules29225259

Denzer, L., Schroten, H., & Schwerk, C. (2020). From Gene to Protein—How Bacterial Virulence Factors Manipulate Host Gene Expression During Infection. *International Journal of Molecular Sciences*, *21*(10), 3730. https://doi.org/10.3390/ijms21103730

Faisal, A., & Arhasy, F. (2025). The Role of Bioinformatics in the Discovery of Traditional Indonesian Medicines for the Treatment of Metabolic Syndrome. *Publication of the International Journal and Academic Research*, *1*(2), 86–93. https://doi.org/10.63222/pijar.v1i2.19

Fajri Ahmad, F., Junita, N., & Nur Aini Yusuf, S. (2022). *Formulasi Dan Uji Aktivitas Antibakteri Sediaan Obat Kumur Ekstrak Etanol Daun Mengkudu (Morinda citrifolia L.) terhadap Bakteri Streptococcus mutans* (Vol. 1, Issue 2). Desember.

Galanis, K. A., Nastou, K. C., Papandreou, N. C., Petichakis, G. N., Pigis, D. G., & Iconomidou, V. A. (2021). Linear B-Cell Epitope Prediction for In Silico Vaccine Design: A Performance Review of Methods Available via Command-Line Interface. *International Journal of Molecular Sciences*, *22*(6), 3210. https://doi.org/10.3390/ijms22063210

Garg, A., & Gupta, D. (2008). VirulentPred: a SVM-based prediction method for virulent proteins in bacterial pathogens. *BMC Bioinformatics*, *9*(1), 62. https://doi.org/10.1186/1471-2105-9-62

Green, E. R., & Mecsas, J. (2016). Bacterial Secretion Systems: An Overview. *Microbiology Spectrum*, *4*(1). https://doi.org/10.1128/microbiolspec.vmbf-0012-2015

Hamidinia, M., Gu, Y., Ser, Z., Brzostek, J., Tay, N. Q., Yap, J., Chua, Y. L., Lim, Y. T., Wood, K. J., Vathsala, A., Sobota, R. M., MacAry, P. A., & Gascoigne, N. R. J. (2025). Occlusion of TCR binding to HLA-A*11:01 by a non-pathogenic human alloantibody. *Cellular and Molecular Life Sciences*, *82*(1). https://doi.org/10.1007/s00018-025-05614-y

Hamka, N. R. Q. P., Jelita, H., & Kahanjak, D. N. (2024). Hubungan Lama Penyakit Ginjal Kronis dengan Kejadian Karies Gigi. *Barigas: Jurnal Riset Mahasiswa*, *2*(1). https://doi.org/10.37304/barigas.v2i1.10445

Kandasamy, P., Gyimesi, G., Kanai, Y., & Hediger, M. A. (2018). Amino acid transporters revisited: New views in health and disease. In *Trends in Biochemical Sciences* (Vol. 43, Issue 10, pp. 752–789). Elsevier Ltd. https://doi.org/10.1016/j.tibs.2018.05.003

Kashyap, D., Khan, A., & Lahare, B. (2020). *Pathogenic Protein Identification and Localization Prediction in Pseudomonas fuscovaginae: A Study on Sheath Brown Rot in Rice*. *XXIX*, 150–160. https://doi.org/10.53555/03276716.2020.20

KEMENKES RI. (2024). *Survei Kesehatan Indonesia*.

Kementerian Pertanian Republik Indonesia. (2024). *Angka Tetap Hortikultura Tahun 2023*.

Kumkar, S. N., Kamble, E. E., Chavan, N. S., Dhotre, D. P., & Pardesi, K. R. (2022). Diversity of resistant determinants, virulence factors, and mobile genetic elements in Acinetobacter baumannii from India: A comprehensive in silico genome analysis. *Frontiers in Cellular and Infection Microbiology*, *12*. https://doi.org/10.3389/fcimb.2022.997897

Lemos, J. A., Palmer, S. R., Zeng, L., Wen, Z. T., Kajfasz, J. K., Freires, I. A., Abranches, J., & Brady, L. J. (2019). The Biology of Streptococcus mutans. *Microbiology Spectrum*, *7*(1). https://doi.org/10.1128/microbiolspec.GPP3-0051-2018

Lyon, P. (2015). The cognitive cell: Bacterial behavior reconsidered. In *Frontiers in Microbiology* (Vol. 6, Issue MAR). Frontiers Media S.A. https://doi.org/10.3389/fmicb.2015.00264

Matsumoto-Nakano, M. (2018). Role of Streptococcus mutans surface proteins for biofilm formation. In *Japanese Dental Science Review* (Vol. 54, Issue 1, pp. 22–29). Elsevier Ltd. https://doi.org/10.1016/j.jdsr.2017.08.002

Nagarajan, S. N., Lenoir, C., & Grangeasse, C. (2022). Recent advances in bacterial signaling by serine/threonine protein kinases. In *Trends in Microbiology* (Vol. 30, Issue 6, pp. 553–566). Elsevier Ltd. https://doi.org/10.1016/j.tim.2021.11.005

Nagasawa, R., Ito, T., Yamamoto, C., Unoki, M., Obana, N., Nomura, N., & Toyofuku, M. (2025). Membrane vesicle production via cell-to-cell communication-induced autolysis in Streptococcus mutans. *Microbiology Spectrum*, *13*(7). https://doi.org/10.1128/spectrum.00334-25

Nawan, N., Handayani, S., & Toemon, A. I. (2025). Bioinformatic Analysis of Dihomo-γ-linolenic Acid (DGLA) Targeting Virulence Factors in Bacteria Causing Infectious Diseases. *Iranian Journal of Medical Microbiology*, *19*(1), 12–28. https://doi.org/10.30699/ijmm.19.1.12

Nawan, N., Priskila, H., Shinta, H. E., Septi Handayani, & Ravenalla Abdurahman. (2023). Quality of the peat water and its association with public health problems in the community of the Danau Tundai area. *Jurnal Kedokteran Dan Kesehatan Indonesia*, 163–171. https://doi.org/10.20885/jkki.vol14.iss2.art7

Noviana, R., Fajrina, A., Eriadi, A., & Asra, R. (2021). Antimicrobial Activity of *Morinda citrifolia L. Asian Journal of Pharmaceutical Research and Development*, *9*(1), 141–148. https://doi.org/10.22270/ajprd.v9i1.924

Raychaudhuri, S. (2010). Recent advances in the genetics of rheumatoid arthritis. *Current Opinion in Rheumatology*, *22*(2), 109–118. https://doi.org/10.1097/BOR.0b013e328336474d

Schooch, C. (2020). NCBI Taxonomy: a comprehensive update on curation, resources and tools. In *Database (Oxford)*.

Soesilawati, P. (2020). *Imunogenetik Karies Gigi*. Airlangga University Press.

Suratri, M. A. L., Jovina, T. A., & Notohartojo, I. T. (2018). Hubungan Kejadian Karies Gigi dengan Konsumsi Air Minum pada Masyarakat di Indonesia. *Media Penelitian Dan Pengembangan Kesehatan*, *28*(3), 211–218. https://doi.org/10.22435/mpk.v28i3.254

Szklarczyk, D., Santos, A., von Mering, C., Jensen, L. J., Bork, P., & Kuhn, M. (2016). STITCH 5: augmenting protein–chemical interaction networks with tissue and affinity data. *Nucleic Acids Research*, *44*(D1), D380–D384. https://doi.org/10.1093/nar/gkv1277

Tadros, D. M., Racle, J., & Gfeller, D. (2025). Predicting MHC-I ligands across alleles and species: how far can we go? *Genome Medicine*, *17*(1). https://doi.org/10.1186/s13073-025-01450-8

Wardana, R. D., Savira, M., Anggraini, D., Amalia, A. S., & Nurulita, Y. (2024). Deteksi Mekanisme Efflux Pump Pada Resistensi Bakteri Staphylococcus haemolyticus, Sampel Pus Klinis Rumah Sakit Pekanbaru. *Chimica et Natura Acta*, *12*(3), 182–192. https://doi.org/10.24198/cna.v12.n3.52038

Yaneva, Z., Beev, G., Rusenova, N., Ivanova, D., Tzanova, M., Stoeva, D., & Toneva, M. (2022). Antimicrobial Potential of Conjugated Lignin/Morin/Chitosan Combinations as a Function of System Complexity. *Antibiotics*, *11*(5), 650. https://doi.org/10.3390/antibiotics11050650

You, Y.-O. (2019). Virulence genes of Streptococcus mutans and dental caries. *International Journal of Oral Biology*, *44*(2), 31–36. https://doi.org/10.11620/IJOB.2019.44.2.31

Zhang, Y.-H., Huang, F., Li, J., Shen, W., Chen, L., Feng, K., Huang, T., & Cai, Y.-D. (2024). Identification of Protein–Protein Interaction Associated Functions Based on Gene Ontology. *The Protein Journal*, *43*(3), 477–486. https://doi.org/10.1007/s10930-024-10180-6

THIS PAGE INTENTIONALLY LEFT BLANK